Texture analysis of land cover change detection

Fen Yang and Roly Lishman

Department of Computing Science, University of Aberdeen, Aberdeen AB24 3UE, UK
Email: fyang@csd.abdn.ac.uk jrl@csd.abdn.ac.uk

Abstract:
We wish to detect land cover change for environmental management. The abilities of Laws Masks and Gabor filters to distinguish land cover types are evaluated since they are common texture measures. This paper investigates a texture based image description in which the standardised MPEG-7 Homogeneous Texture Descriptors (HTD) of Gabor filters are used as the textural feature vector. A discriminant classifier is designed to use linear regression analysis to distinguish vectors derived from the filter images. Experiment results show that both Laws Masks and Gabor filters are capable of expressing texture information of land covers, but they have different results on different land cover types.

Key Words

Change detection, discriminant analysis, Gabor filters, Laws Masks, texture classification, remote sensing

1. Introduction

Land use and land cover are important aspects in studying environmental changes. Since it is a large burden for human photo-interpreters to classify landscape or detect change from remotely sensed images, many automatic and semi-automatics methods have been applied to this area. As a kind of spatial description, texture provides context information to describe images. In landscape images most of land covers contain variations of intensities which form certain repeated patterns, *i.e.* visual textures. The patterns could be the result of physical surface properties such as roughness or orientation which often have a perceivable quality, or they could be the result of reflectance differences. Therefore, employing texture information in land use/cover becomes more popular, and the results become better (Harris and Ventura 1995).

Texture can be perceived when people see it but it is very difficult to define. There is no uniform definition for it. However, most of researchers agree that an image of visual texture should be spatially homogeneous, and typically contains repeated structures, often with some random variations (*e.g.* random positions, orientations or colours). As early as 1973, Haralick (1973) applied statistical textures to classify remotely sensed images. Based on Haralick(1973)'s research, many researchers(Rajesh *et al.* 2001, Smits and Annoni 1999, Bevk and Kononenko 2002) made use of co-occurrence matrics to land use/cover application. Many kinds of texture measures are applied to this area. Xiao *et al.* (2002) applied wavelet based texture features to land cover change detection, but the land covers in the experiments only involved 5 classes. Dutra *et al.* (2000) applied Laws Masks to distinguish undulated and flat forest. There are many kinds of texture measures in image processing. However, texture measures used in land use/cover application focus on statistical textures and co-occurrence matrices. Although those texture measures achieve better results than those only applying spectral information, the applications limit to specific types of land cover and the parameters are tricky to understand and use.

Texture measures can be extracted in spatial space or spatial frequency space. The extracting way depends on the specific application. The landscape image is complex and contains various land cover types. These land cover types have versatile shapes and appearances. Even the same kind of land cover type appears different. For example, Figure. 1 shows two ploughed fields with furrows of different width and direction. The fact that various types of land cover have various spatial distributions implies that attempting to find texture measures for all land cover types is hard. Most researchers concentrate on a few types of land cover. Therefore, it is worth investigating the ability of texture measures to capture differences of various land covers and distinguish them. In this paper, two kinds of texture measures, Gabor filters and Laws masks, are used as texture feature vectors to discriminate different

land covers. While texture information extracted by Laws masks are from spatial domain, Gabor filters extract them from spatial frequency domain.

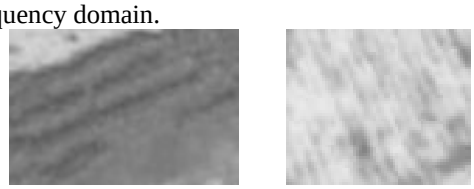

Figure 1. Same type of land cover appears different. These two are both labelled as recent ploughed field. Traces have different directions and those in left one are wider than those in right one.

This paper is organised as follows: Laws Masks are introduced in part 2. Gabor filters and MPEG-7 texture descriptors are reviewed in part 3. In part 4 a discriminant classifier based on the linear regression analysis examines these two texture measures' distinguishing abilities. The final part describes the experiment design and the conclusions.

2. Laws Masks

A kind of common approach to generating texture feature is to use local masks to capture local information in images. Laws (1980) developed a texture-energy approach that measures the amount of variation within a fixed-size window. He defined a set of 5*5 convolution masks to compute texture energy, which is then represented by a vector for each pixel of the image being analysed. These vectors are the convolution results of masks and the image. The masks are achieved through the following vectors.

$$
\begin{aligned}
L5 \quad (Level) &= \begin{vmatrix} 1 & 4 & 6 & 4 & 1 \end{vmatrix} \\
E5 \quad (Edge) &= \begin{vmatrix} -1 & -2 & 0 & 2 & 1 \end{vmatrix} \\
S5 \quad (Spot) &= \begin{vmatrix} -1 & 0 & 2 & 0 & -1 \end{vmatrix} \\
R5 \quad (Ripple) &= \begin{vmatrix} 1 & -4 & 6 & -4 & 1 \end{vmatrix}
\end{aligned}
$$

These vectors imitate four different spatial distributions. And like the names meaning, the *L5* vector gives a centre-weighted local average. The *E5* vector detects edges, the *S5* vector detects spots, and the *R5* vector detects ripples. The 2D convolution masks are obtained by computing outer products of pairs of vectors. For example, the mask *L5E5* is computed as the product of *L5* and *E5* as:

$$
\begin{bmatrix} 1 \\ 4 \\ 6 \\ 4 \\ 1 \end{bmatrix} \times \begin{bmatrix} -1 & -2 & 0 & 2 & 1 \end{bmatrix} = \begin{bmatrix} -1 & -2 & 0 & 2 & 1 \\ -4 & -8 & 0 & 8 & 4 \\ -6 & -12 & 0 & 12 & 6 \\ -4 & -8 & 0 & 8 & 4 \\ -1 & -2 & 0 & 2 & 1 \end{bmatrix}
$$

These masks can measure different contents of the images. For example, *E5L5* measures horizontal edge content, and *L5E5* measures vertical edge content. Because some masks are symmetric, they are combined and replaced by the average. Finally only nine masks are used to extract texture measures. They are

L5E5/E5L5	*L5S5/S5L5*
L5R5/R5L5	*E5E5*
E5S5/S5E5	*E5R5/R5E5*
S5S5	*S5R5/R5S5*
R5R5	

These masks are subsequently convolved with the image to accentuate its microstructure which generates the energy map. Nine energy maps are obtained for every image. Let $F_k[i, j]$ be the result of filtering with the kth mask at pixel $[i.j]$. Then the texture energy map E_k for filter k is defined by

$$E_k[r,c] = \sum_{j=c-7}^{c+7} \sum_{i=r-7}^{r+7} |F_k[i,j]| \qquad (1)$$

Where *(r,c)* is the centre point of the filtering window. The size of the window depends on the class of imagery. A 15*15 window is used for natural scenes (Shapiro and Stockman 2001). Each texture energy map is a full image, representing the application of the kth mask to the input image. Statistical measures, *i.e.* mean, standard deviation, skewness, kurtosis and energy, are regarded as texture measures and form a vector for future classification.

3. Gabor Filters

Gabor filters are another kind of operator that can capture the local information in an image optimally. And research show that Gabor filters mimic the biological perception of texture and share many properties with the human visual system (Raghunathan and Acton 2000). The properties of Gabor filters make them capable of reaching the minimum bound for simultaneous localisation in the spatial and spatial/frequency domains (Manthalkar *et al.* 2002). Gabor filters can be calculated at different spatial frequencies so can capture similarities in images of different scales.

3.1 Gabor Functions

A Gabor function is a complex sinusoid modulated by a Gaussian envelope. Its general form of one dimension in Cartesian co-ordinate is:

$$g(x) = \frac{1}{\sqrt{2\pi}\sigma} \cdot \exp(\frac{-x^2}{2\sigma^2}) \cdot \exp(i2\pi \frac{x}{\lambda}) \qquad (2)$$

where σ, the standard deviation of the Gaussian function, determines the size of the receptive field. λ is the wavelength of the complex sinusoid. $2\pi/\lambda$ determines the preferred spatial frequency of the receptive field function.

The 1-D Gabor function of Cartesian co-ordinate in the spatial frequency domain is as follows:

$$G(u) = \exp\left[\frac{-\sigma^2(u-u_c)^2}{2}\right] \qquad (3)$$

where u is the spatial frequency and u_c is the preferred spatial frequency with value $2\pi/\lambda$ as defined above.

The 1-D Gabor function may be extended to 2-D as follows:

$$g(x,y) = \frac{1}{2\pi\sigma^2} \cdot \exp\left[-\frac{1}{2}\left(\frac{x^2+y^2}{\sigma^2}\right)\right] \cdot \exp[i2\pi(\frac{x+y}{\lambda})] \qquad (4)$$

where σ and λ are defined as above. Its spatial frequency domain in Cartesian co-ordinate is given by:

$$G(u,\upsilon) = \exp\left[\frac{-\sigma^2(u-u_c)^2}{2}\right] \cdot \exp\left[\frac{-\sigma^2(\upsilon-\upsilon_c)^2}{2}\right] \qquad (5)$$

where u and υ are spatial frequencies along the x and y axis, and u_c and υ_c are the selected spatial frequencies along the x and y directions respectively.

If we let f denote the radial frequencies and θ denote orientations, above 2D Gabor function in the spatial frequency domain could be expressed in polar co-ordinate. Haley and Manjunath (1999) pointed that compared with the standard form, the Gabor function in polar form has a narrower response at low frequencies and a wider response at high frequencies. This makes a more uniform coverage of the

frequency domain with less overlap at low frequencies and smaller gaps at high frequencies. Also the polar form is more suitable for rotation invariant analysis which is a requirement to describe natural objects in landscape images. Another advantage of the polar form is that the parameters of Gabor function are more easily determined than the standard form. The Gabor function in polar form will be described in next part.

3.2 MPEG-7 Homogeneous Texture Descriptor

MPEG-7, the Multimedia Content Description Interface, is an ISO/IEC standard for describing the multimedia content, developed by MPEG (Moving Picture Expert Group) (MPEG homepage). It describes three texture descriptors, a homogeneous texture descriptor (HTD), an edge histogram descriptor (EHD), and a perceptual texture browsing descriptor (PBD).

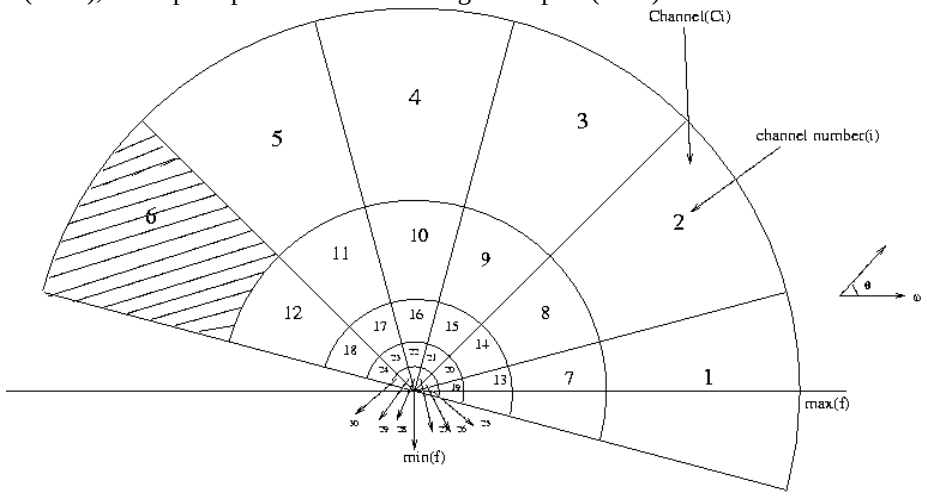

Figure 2. Frequency partition of the Gabor filter bank with ID's of the feature channels C in the spatial frequency domain. $\max(f)$ and $\min(f)$ denote the maximum and minimum frequency in the spatial frequency domain respectively.

The HTD provides a precise quantitative representation of texture that is useful for similarity analysis. The descriptor is derived from filtering with original image using scale and orientation selective kernels which create a filter bank. Gabor functions in the spatial frequency domain in polar form make them convenient to generate the parameters of Gabor kernels. The Spatial frequency domain in polar co-ordinate could be partitioned into 30 channels with equal divisions in the angular direction (at 30° intervals) and octave division in the radial direction (five octaves), as shown in Fig. 2 taken from (Manjunath *et al.* 2001). The channel index i can be denoted as $i = 6 * s + r + 1$. Here s is the radial index with $s \in \{0,1,2,3,4\}$ and r is the angular index with $r \in \{0,1,2,3,4,5\}$.

Every feature channel in the spatial frequency domain is modelled using a 2-D Gabor function of polar form as follows:

$$G_{P_{s,r}}(f,\theta) = \exp\left[\frac{-(f-f_s)^2}{2S_{f_s}^2}\right] \cdot \exp\left[\frac{-(\theta-\theta_r)^2}{2S_{\theta_r}^2}\right] \qquad (6)$$

where f is the frequency in radial direction. θ is the angular direction. Centre frequency of octave bandwidth $f_s = \frac{3}{4} \cdot (\max(f) - \min(f)) \cdot 2^{-s}$, where radial index $s \in \{0,1,2,3,4\}$. $\max(f)$ is the maximum frequency of the image and has wavelength 2 pixels/cycle. $\min(f)$ is the minimum frequency of the image and has wavelength 1 picture/cycle. Angular direction $\theta_r = 30^\circ * r$, where angular index $r \in \{0,1,2,3,4,5\}$. S_{f_s} and S_{θ_r} are the standard deviations of the Gabor function in

the radial direction and the angular direction respectively. In the angular direction, S_{θ_r} has a constant value as follows:

$$S_{\theta_r} = \frac{15°}{\sqrt{2\ln 2}} \qquad (7)$$

In the radial direction, S_{f_s} depends on the octave bandwidth as follows:

$$S_{f_s} = \frac{B_s}{2\sqrt{2\ln 2}} \qquad (8)$$

where B_s is the octave bandwidth whose value is $(\max(f) - \min(f)) \cdot 2^{-(s+1)}$.

The HTD generates a feature vector TD constituted by the mean value f_{DC} and standard deviation f_{SD} of the original image as well as the energies e_i and their standard deviations d_i of the Gabor filtered images.

Table 1. Parameters of the Gabor Filter Bank in the radial direction. Frequency range $f_0 = \max(f) - \min(f)$. f is the frequency variable of the original image.

Radial Index S	0	1	2	3	4
Centre Frequency f_s	$3/4 * f_0$	$3/8 * f_0$	$3/16 * f_0$	$3/32 * f_0$	$3/64 * f_0$
Octative Bandwidth B_s	$1/2 * f_0$	$1/4 * f_0$	$1/8 * f_0$	$1/16 * f_0$	$1/32 * f_0$

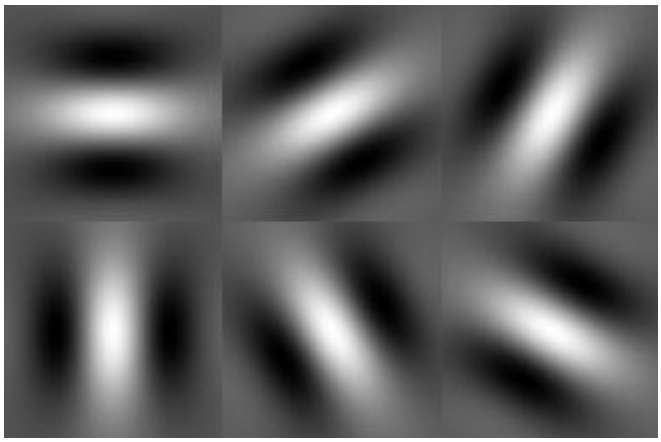

Figure 3. Six 128*128 Gabor filters in spatial space whose center frequencies are at 3/32* f_0. Bandwidth is 1/16* f_0 and angular directions are $0°$, $30°$, $60°$, $90°$, $120°$, $150°$.

$$TD = [f_{DC}, f_{SD}, e_1, e_2, e_3, \cdots, e_{30}, d_1, d_2, d_3, \cdots d_{30}] \qquad (9)$$

3.3 Parameters of Gabor Filters

The parameters of Gabor filters are obtained by the partition of the space frequency domain in the way described above. The radial parameters are shown in Table 1. The frequency range f_0 is chosen as 64 since frequencies of most land covers are not bigger than it. The angle directions in Gabor filters are from $0°$ to $150°$. Six Gabor filters in scale of 3 changing with the whole angular directions are shown in Figure 3.

4. Discriminant Analysis

Discriminant analyses (DA) is a supervised classification method, which is used to build a predictive model of group membership based on observed characteristics of each case. A discriminant function or a set of discriminant functions if there are more than two groups, is generated based on linear combinations of the feature vectors. The discriminant functions are generated from a sample of cases for which group memberships are known, and the functions can then be applied to new cases with measurements for the independent variables but unknown group membership. The discriminant function is defined as follows:

$$L = B \cdot TD_1^{'} \qquad (10)$$

where B is the vectr of discriminant coefficients. These discriminant coefficients try to maximise the distance between the means of the variables in derived texture vectors. $TD_1^{'}$ is the transpose of TD_1 which is from feature vector obtained from Laws masks and Gabor filters. So how to find an effective way to decide discriminant coefficients?

Linear regression explores the relationship between independent variables and what you want to predict. So it can be used to distinguish two groups. Thus discriminant functions are estimated by linear regression. The linear regression coefficients become the discriminant coefficients and are derived by least square minimisation. Group membership can then be determined by the discriminant score calculated with the linear regression function. There is a dividing point $\bar{D}$

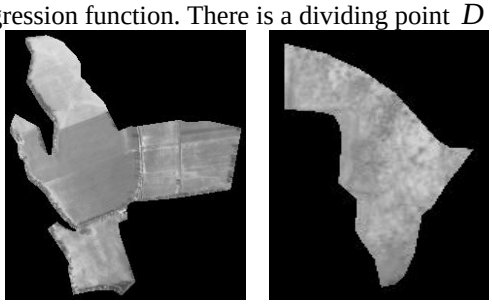

Figure 4. Left polygon is labelled as arable field, and right polygon is labelled as smooth grass/rushes.

to determine the membership of new case.

$$\bar{D} = \frac{\bar{D}_1 + \bar{D}_2}{2} \qquad (11)$$

where $\bar{D}_1$ and $\bar{D}_2$ are means of discriminant scores of cases which have known the group memberships in group 1 and group 2 respectively.

If discriminant score is less than $\bar{D}$, the new case has to be assigned to the first group, otherwise it is assigned to the other group.

5. Experiments and Results

Ten kinds of land cover types have been tested, as these land cover types are ecologically “similar”. From the Table 2 it is clear that under every type, there are more detailed subclasses. The work of

Comber (2002) presents predictions about possible changes of land cover over time and excludes impossible ecological changes, such as bare rock can not change to ploughed fields. Possible changes are shown in Table 2. With this guidance, we need only distinguish possible successor covers from the original. In this experiment training and testing data are used half-and-half to avoid bias.

5.1 Description of the Used Image Data

The data in this experiment is from aerial images covering the Elgin area in north-east Scotland. The image has been manually segmented into different land cover types by expert interpreters who gave every pixel in the image a land code representing the land cover type of the pixel. To detect land cover changes a classifier has to be designed to discriminate various land cover types. Images only containing a single land type are required to be prepared so that different information from different land cover types could be compared and analysed without the influence of other land cover types. According to the given code polygons with single land cover are obtained by using the floodfill method. Finally the image covering Elgin has been split into many polygons. Fig. 4 shows two examples of polygons produced by the floodfill method. There may exist many polygons associated with one land cover code because polygons with the same land cover code may not be adjacent. Thus it is ready to derive land cover texture information from these different polygons for further analysis.

5.2 Experiment Results

There are a total of 475 polygons of 10 land types used in the experiment. Fig. 5 shows an example of some textures used in the training dataset. According to the method mentioned above polygons obtained from floodfill method are correlated with 9 Laws Masks and 30 Gabor filters respectively. Texture features are derived from the filtered images, and then input to a linear regression discriminant classifier. SPSS, a statistical software package, is used to help determine the discriminant coefficients. The classification result of these two texture measures is shown in Fig 6. In which the classification rates of the texture measures in different ranges are compared.

Results show that these two kinds of texture measures are promising to detect land cover changes. Most of the correct classification rates are higher than 80%. The correct classification rate in training data is better than it in testing data. It implies that more data is required in the training stage to obtain parameters for the discriminant classifier. Although it shows that Gabor filter is a little better than Laws mask to tell these 10 land covers, the abilities of different texture measures to describe land covers are different. Due to the complexity of land covers, applying more than one texture measure is more reasonable. It is better to examine the abilities of different texture measures and choose the one with the best performance when dealing with complex land cover images.

Acknowledgements

The authors would like to acknowledge Macaulay Land Use Research Institute for providing the mosaic images.

References

Bevk, M., Kononenko, I., July 2002. A statistical approach to texture description of medical images: A preliminary study. In: ICML Workshop on Machine Learning in Computer Vision. Sydney, Australia.

Comber, A., 2002. Automated land cover change detection. Ph.D. thesis, University of Aberdeen, University of Aberdeen, King's College, Aberdeen AB24 3FX, Scotland.

Dutra, L. V., Huber, R., Soares, S. M., 2000. Forest classification from SAR data using multiresolutional and autogressive approaches. In: Proceedings of World Multiconference on Systemics, Cybernetics and Informatics. Vol. V, Part I, pp419-423, USA.

Fukuda, S., Hirisawa, H., September 1999. A wavelet-based feature set applied to classification of multifrequency polarimeter SAR images. In: IEEE Transaction. On Geoscience and Remote Sensing. Vol. 37. pp. 2282-2286.

Haralick, R. M., Shanmugam, K., Dinstein, I., 1973. Texture features for image classification. IEEE Transaction on Systems, Man, and Cybernetics 3 (6), 610-621.

Haley, G. M., and Manjunath, B. S., 1999. Rotation-invariant texture classification using a complete space-frequency model. In IEEE Transactions On Image Processing, Vol. 8, February 1999, pp. 255-269.

Harris, P., Ventura, S., 1995. The integration of geographic data with remotely sensed imagery to improve classification in an urban area. Photogrammetric Engineering and Remote Sensing 61, 993-998.

Kurosu, T., Uratsuka, S., Maeno, H., Kozu, T., Jan. 1999. Texture statistics for classification of land use with multitemporal JERS-1 SAR single-look imagery. In: IEEE Transaction. On Geoscience and Remote Sensing. Vol. 37. pp. 227-235.

Kurvinen, L., Hallkainen, M. T., March 1999. Texture information of multitemporal ERS-1 and JERS SAR images with application to land and forest type classification in boreal zone. In: IEEE Transaction. On Geoscience and Remote Sensing. Vol. 37. pp. 680-689.

Laws, K. I., 1980. Textured image segmentation. Ph.D. thesis, University of Southern California.
Manjunath, B. S., Ohm, J. R., Vasudevan, V. V., and Yamada, A., 2001. Colour and Texture Descriptors, in IEEE Transaction on Circuits and Systems for Video Technology, vol. 11, June 2001, pp. 703-715.

Manthalkar, R., Biswas, P. K., and Chatterji, B. N., 2002. Rotation and scale invariant texture classification using Gabor Wavelets, in Proceeding of 2nd Texture Workshop, Copenhagen, Denmark.
MPEG-7, 2002.The MPEG Homepage[Online]. Available: http://mpeg.telecomitalialab.com. Accessed in March 2002.

Raghunathan, B. and Acton, S. T., 2000. Content Based Retrieval for Remotely Sensed Imagery, in Proceedings of IEEE Southwest Symposium on Image Analysis and Interpretation, Austin, USA.

Rajesh, K., Jawahar, C., Sengupta, S., Sinha, S., 2001. Performance analysis of textural features for characterization and classification of SAR images. International Journal of Remote Sensing 22 (8), 1555-1569.

Shapiro, L. G., Stockman, G. C., 2001. Computer Vision. Prentice-Hall Inc., New Jersey 2001.

Smits, P., Annoni, A., May 1999. Updating land-cover maps by using texture information from very high-resolution space-borne imagery. IEEE Transcations on Geoscience and Remote Sensing 37 (3), 1244-1254.

Xiao, P., Zhao, X., Li, D., 2002. Land use/cover change detection based on artificial neural networks and wavelet based texture analysis. In: Proceedings of the ISPRS Technical Commission II Symposium 2002, Xi'an, P.R.China. pp535-540.

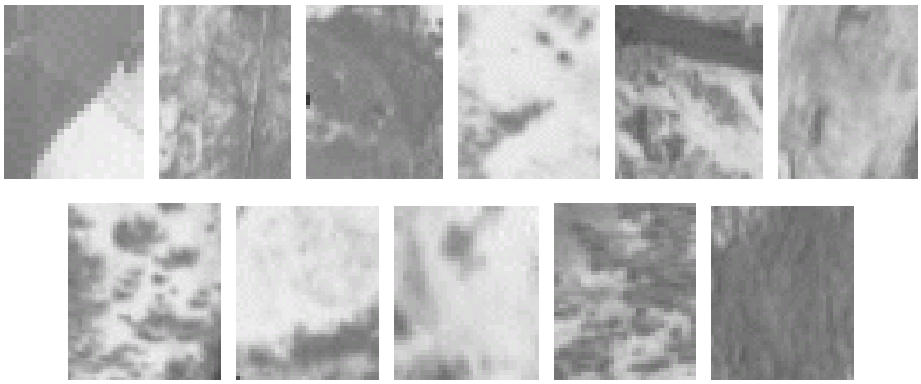

Figure 5. An example of textures in training data set. From left to right and up to down, the land cover code of these polygons are: 100, 150, 151, 155, 156, 160, 161, 140, 170, 79, and 82 as denoted in tab. 2

Table. 2 A Transition Matrix shows natural ecological trends if management was removed.

0=unlikely 1=possible 2=likely (From)	Main features	codes	(To)	Arable 1	Good rough grassland 2	Heather moorland 3	Poor rough grassland 4	Bracken 5	Mixed woodland 6	Scrub 7	Peatland 8	Semi-natural coniferous 9	Broadleaved 10
Arable	Arable land	100	1		2		1	1	1	1			1
Good rough grassland	Smooth G(rushes, crub,undiff.)	150,151,155,156,160,161	2				1	2	1	2			1
Heather moorland	HM(wet, dry undiff.)	110,111,112,120,130, 131,132	3					1	2	2	1	2	2
Poor rough grassland	Undiff. Coarse G	140	4			1		1		1			1
Bracken	Undiff. Smooth G with bracken	170	5						1	2			1
Mixed woodland	Undiff. Mixed woodland(area)	79	6							1			1
Scrub	Undiff. Low scrub	82	7						1			1	2
Peatland	Blanket bog	180,182,183,186	8			1	1			1			
Semi-natural coniferous	Semi-nat conif woodland	73	9						1	1			
Broadleaved	Broadleaved W	76	10							1			

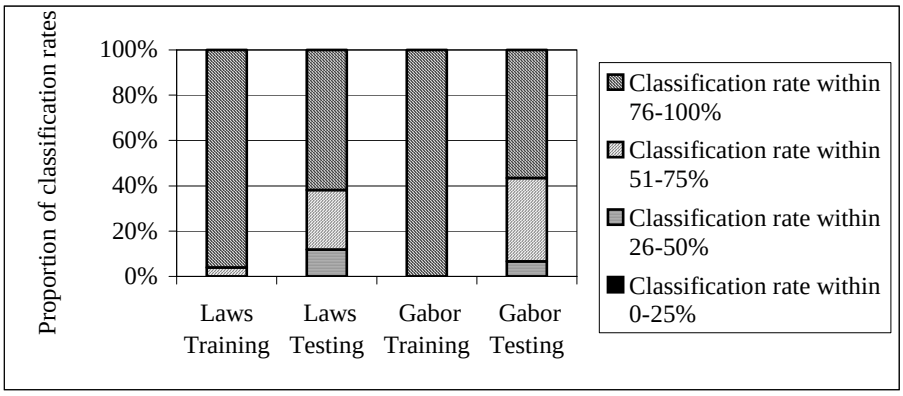

Figure 6. Comparison of performances of Laws Masks and Gabor Filters in different classification rate ranges.